Catalysis Science & Technology

PAPER

View Article Online
View Journal

Cite this: DOI: 10.1039/c4cy01376j

Renewable fuels from biomass-derived compounds: Ru-containing hydrotalcites as catalysts for conversion of HMF to 2,5-dimethylfuran†

Atul S. Nagpure, Ashok Kumar Venugopal, Nishita Lucas, Marimuthu Manikandan, Raja Thirumalaiswamy* and Satyanarayana Chilukuri*

Received 20th October 2014,
Accepted 25th November 2014

DOI: 10.1039/c4cy01376j

www.rsc.org/catalysis

Production of transportation fuels from renewable biomass is hugely important considering the current ecological concerns over CO_2 built up in the atmosphere. Ruthenium-containing hydrotalcite (HT) catalysts were applied for the selective hydrogenolysis of biomass-derived 5-hydroxymethylfurfural (HMF) to 2,5-dimethylfuran (DMF). Structural and morphological features of the catalysts were examined using various physico-chemical characterization techniques. The influence of various reaction parameters, such as reaction temperature, solvent, Ru content of the catalyst, *etc.*, was investigated with respect to HMF conversion and DMF yield. The study clearly shows that well-dispersed Ru nanoparticles are highly active and selective in the conversion of HMF to DMF. A catalyst containing only 0.56 wt% Ru converted 100 mol% HMF to yield 58 mol% DMF. This catalyst was found to be recyclable as the activity was retained even after five cycles of reaction. 2-Propanol was found to be a good solvent as it helped to improve DMF yield through transfer hydrogenation. Based on the results of the investigations, a reaction pathway for the conversion of HMF to DMF was proposed for the present Ru-based catalyst system.

1. Introduction

At present, there is an alarmingly heavy dependence on fossil fuels, which is not sustainable. Moreover, their indiscriminate use is leading to ecological problems. Hence, utilization of biomass to produce renewable fuels and valuable chemical intermediates is gaining increasing attention.[1–4] Hydrogenolysis is an important process in biomass refinement, as biomass-derived materials have high oxygen content.[5,6] 5-Hydroxymethylfurfural (HMF), an important platform chemical that can be synthesized from hexoses, has been identified as a key player in the bio-based renaissance. It can be converted to levulinic acid, ethyl levulinate, γ-valerolactone and the highly promising transportation fuel additive 2,5-dimethylfuran (DMF).[7–12] DMF is particularly attractive due to its superior energy density (30 kJ cm^{-3}), high research octane number (RON = 119) and ideal boiling point (92–94 °C).[8] Further, DMF is immiscible with water and also easier to blend with gasoline compared to ethanol. Biomass-derived DMF has been tested as a biofuel in a single-cylinder gasoline direct-injection research engine.[13] The performance of DMF was satisfactory against gasoline in terms of ignition, emission and combustion characteristics. These attributes bode very well for the use of DMF as an alternative fuel for transportation.

There were several recent reports on the conversion of biomass to DMF. Dumesic and co-workers utilized a two-step process to convert fructose to DMF.[8] The first step involved the dehydration of fructose to HMF using HCl in a biphasic solvent system, followed by vapor-phase hydrogenolysis of HMF to DMF, using a Cu–Ru/C catalyst. Thananatthanachon and Rauchfuss showed a milder pathway for the production of DMF using formic acid as a reagent and Pd/C as a catalyst.[14] Formic acid functioned as a hydrogen donor during the second step and also assisted in the deoxygenation of HMF to DMF. To get a high yield of DMF, formic acid and H_2SO_4 have to be used simultaneously. But, both acids are not environmentally friendly. Chidambaram and Bell used Pd/C as a catalyst in ionic liquids to convert 47 mol% HMF, yielding 15 mol% DMF.[15] A potential drawback of this method is the low solubility of H_2 in ionic liquids. As a result, a high pressure of H_2 (62 bar) has to be used, making the process highly energy intensive.

Catalysis Division, CSIR - National Chemical Laboratory, Dr. Homi Bhabha Road, Pune-411008, India. E-mail: sv.chilukuri@ncl.res.in, t.raja@ncl.res.in; Fax: +91 20 25902633; Tel: +91 20 25902019

† Electronic supplementary information (ESI) available. See DOI: 10.1039/c4cy01376j

Hansen *et al.* reported the catalytic transfer hydrogenation (CTH) of HMF over Cu-containing mixed metal oxides using supercritical methanol that yielded 48 mol% DMF.[16] Gallo *et al.* studied the hydrogenolysis of HMF in the presence of lactones using a RuSn/C catalyst to obtain DMF yields up to 46 mol%.[17] Yang and Sen reported the conversion of biomass-derived carbohydrates to 2,5-dimethyltetrahydrofuran (DMTHF), an alternative fuel that can be obtained by further hydrogenation of DMF, using homogeneous $RhCl_3$ and $RuCl_3$ catalysts.[18,19] The same research group has also reported the synthesis of 5-methyl furfural (MF) from fructose using heterogeneous Pd/C as a catalyst.[20] Morikawa *et al.* studied the CTH of HMF using cyclohexane over $AlCl_3$ and Pd/C catalysts with a DMF yield of 60 mol%.[21] These CTH routes, however, have several disadvantages including the use of mineral acids as co-catalysts to enhance hydrogenation activity.[14,22,23]

Recently, it was suggested that the use of catalysts with a high amount of precious metal is not conducive to the overall process economics of the production of liquid transportation fuels from biomass-derived compounds.[24] Commercial application of the HMF to DMF process will be feasible only by developing a strategy that minimizes the precious metal content of the catalyst. The Ru-based catalysts are known for their effectiveness in the hydrogenolysis of polyols to alkanes.[25,26] Hence, in the present report we have demonstrated for the first time, the efficiency of a Ru-doped hydrotalcite (HT) catalyst with very low (0.56 wt%) Ru content for the hydrogenolysis of HMF to DMF. This catalyst showed high catalytic activity and DMF selectivity, in addition to its excellent reusability for the conversion of HMF to DMF. The effect of various reaction parameters on the performance of the catalyst was also investigated by varying the solvent, reaction temperature, H_2 pressure and the Ru metal content in the catalyst. These Ru-based HT catalysts have significant potential for further development and are expected to pave the way for realising the goal of renewable liquid fuels from biomass.

2. Results and discussion

2.1. Structural and morphological characteristics of the catalysts

The structural, textural and morphological characteristics of the as-synthesized Ru-doped HT samples (RH-1, RH-2 and RH-3) along with the corresponding HT precursors were investigated. Fig. 1a shows the XRD profiles of the as-synthesized samples, which have characteristic peaks belonging to pure HT ($d_{(003)}$ = 7.65 Å). No extraneous peaks belonging to other phases (JCPDS no. 70-2151) were seen. These results show that Ru may be present in the brucite-like lattice of HT, as no peaks corresponding to any of ruthenium or its oxide phases were seen. The intensities of reflections pertaining to the layered structure decreased with increasing Ru content of the sample. The XRD patterns of the calcined–reduced Ru-doped HT-derived catalysts (RH-1, RH-2 and RH-3) are given in Fig. 1b, which also includes the spectra of the Ru-impregnated sample (RH-imp). The RH-imp sample has

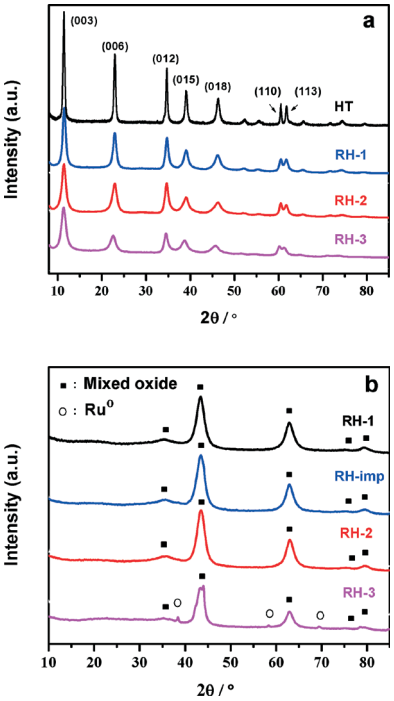

Fig. 1 X-ray diffractograms of (a) the as-synthesized precursors and (b) the calcined–reduced catalysts.

Ru content similar to that of RH-1. The reflections belonging to the periclase phase of Mg(Al)O (JCPDS no. 4-829) were seen predominantly. In addition to the mixed metal oxide phase, metallic Ru peaks were also present in the case of the catalyst with higher Ru content (RH-3). The BET surface areas of calcined HT (HT_{cal}) and calcined–reduced Ru-containing catalysts are given in Table 1. The surface areas of HT_{cal}, RH-1, RH-2, RH-3 and RH-imp were 210, 194, 180, 142 and 185 $m^2\ g^{-1}$, respectively. The surface area decreased with increasing Ru content of the sample, when compared to HT_{cal}. The decrease in surface area may either be attributed to the poor crystallinity, as reflected in lower XRD intensities (Fig. 1), or to the blockage of pores by the segregated Ru oxide phases of the sample.[27]

The morphologies of the HT and Ru-doped HT precursors were investigated by SEM. Some of their representative images are shown in Fig. 2. The micrographs demonstrate the flower-like morphology[28] of parent HT, which has not changed even after Ru incorporation. Dispersion of Ru in the Ru-containing catalysts was investigated by H_2 chemisorption. The Ru metal dispersion, average crystallite size and metal surface areas are included in Table 1. The metal dispersions were: RH-1, 47.6%; RH-2, 33.1%; RH-3, 10.3% and RH-imp, 32.4%. Good Ru dispersion in the RH-1 catalyst (47.6%) confirms the homogeneous distribution of Ru on the metal oxide support with an average Ru crystallite size of 2.8 nm (Table 1). The Ru particle sizes as well as its distribution were also investigated by TEM. These results are shown in Fig. 3. The micrograph of RH-1 shows that Ru nanoparticles are in the 2–6 nm range, dispersed over the

Table 1 Chemical composition and structural characteristics of the catalysts

Catalyst[a]	Synthesis composition Mg : Al : Ru	Ru content[b] (wt%)	BET surface area[c] (m^2 g^{-1})	Ru metal dispersion[d] (%)	Average Ru crystallite size[d] (nm)	Average Ru particle size[e] (nm)	Ru metal surface area[d] (m^2 g^{-1})
HT_{cal}	3 : 1 : 0	0	210	—	—	—	—
RH-1	3 : 0.97 : 0.03	0.56	194	47.6	2.8	3.1	0.97
RH-2	3 : 0.94 : 0.06	1.0	180	33.1	4.0	4.3	1.20
RH-3	3 : 0.90 : 0.10	1.7	142	10.3	12.9	14.0	0.56
RH-imp[f]	3 : 0.97 : 0.03	0.58	185	32.4	4.1	—	1.18

[a] Catalyst precursors prepared by co-precipitation. [b] Estimated by ICP-OES. [c] Calcined–reduced samples. [d] Determined by H_2 chemisorption. The catalysts were calcined at 450 °C and reduced at 350 °C for metal dispersion studies. [e] Calculated based on the surface area averaged TEM particle size. [f] Prepared by the dry impregnation method.

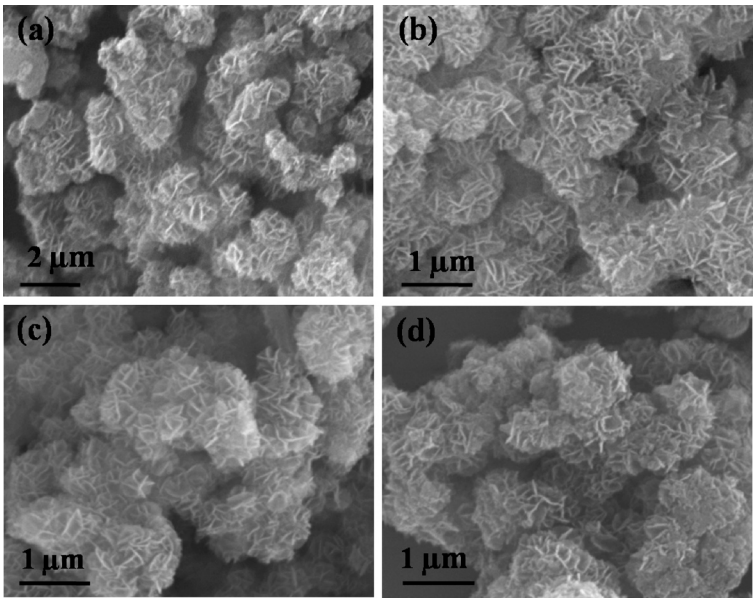

Fig. 2 SEM images of as-synthesized (a) HT, (b) RH-1, (c) RH-2 and (d) RH-3 catalyst.

HT-derived metal oxide support. The average particle size of Ru was 3.1 nm, calculated through the surface area averaged TEM particle size by assuming that the Ru particles are hemispherical in shape, with the flat side on the support. These values for the three catalysts, RH-1, RH-2 and RH-3, are in close agreement with the values obtained from H_2 chemisorption (Table 1; Table S1, ESI†).

Temperature-programmed reduction (TPR) studies helped to understand the reducibility of the Ru supported on mixed oxides. TPR profiles (Fig. 4) showed two H_2 consumption

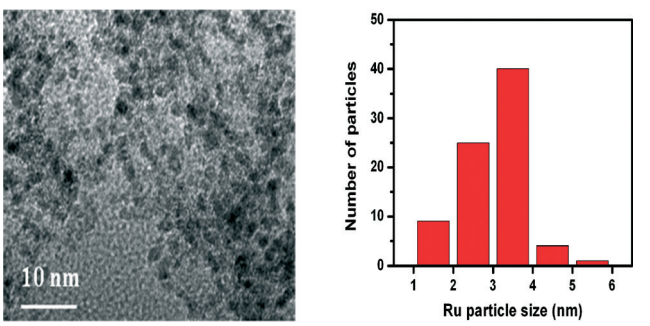

Fig. 3 TEM micrograph and Ru particle size distribution of the RH-1 catalyst.

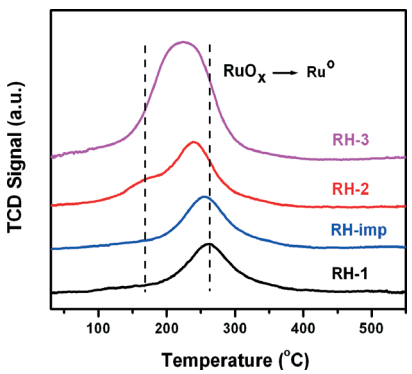

Fig. 4 TPR profiles of various Ru catalysts.

peaks. The first reduction peak is in the range of 120–190 °C, while the second is in the 200–330 °C range. These peaks must be due to the different interactions of the RuO_x species with the support.[29] The low temperature peak is probably due to the weak interaction of Ru with the support, while the high temperature peak may be due to the stronger interaction of Ru with the support. In the case of RH-1, the intensity of the low temperature peak was weak. But, its intensity enhanced with increasing Ru content, implying that the concentration of loosely bound Ru increased. There is also a shift of the high temperature peak towards low temperature at high Ru content, particularly in the case of the impregnated catalyst. In the case of the RH-imp sample, both low and high temperature peaks have merged.

2.2. Catalytic activity in hydrogenolysis of HMF to DMF

2.2.1. Effect of reaction temperature. The influence of reaction temperature on HMF conversion and DMF yield over the RH-1 catalyst was systematically investigated by varying the reaction temperature in the 180–230 °C temperature range. The HMF conversions and DMF yields are shown in Fig. 5 and 6, respectively. It can be clearly seen (Fig. 5) that the temperature played an important role with regard to HMF conversion, as it has increased with increasing reaction temperature. In addition, HMF conversion also increased with reaction time. After 4 h of reaction, HMF conversion increased from 70 to 100 mol%, as the reaction temperature increased from 180 to 210 °C. On the other hand, complete conversion of HMF could be seen within 2 h of the reaction, when the reaction was carried out in the 220–230 °C temperature range. Moreover, the reaction temperature has a profound influence on DMF yield, as may be seen in Fig. 6. The DMF yield increased continuously as a function of reaction time, when the reaction temperature was raised from 180 to 210 °C, indicating that intermediates like 2,5-bis(hydroxymethyl)furan (BHMF), 5-methyl furfuryl alcohol (MFA) and MF that formed during the course of the reaction were converted to DMF with increasing reaction temperature as well as with reaction time.[8,15] On further increasing the reaction temperature to 220 °C, a high DMF yield of 58 mol% could be reached after 4 h of reaction time. But, the DMF yield has decreased on further increasing the reaction time (Fig. 6 and entry 3, Table 3). This decrease in the DMF yield could be attributed to its ring hydrogenation, leading to the formation of DMTHF. The DMF yield decreased continuously at higher reaction temperature (230 °C), which clearly implies that the ring hydrogenation is predominant at higher reaction temperatures (entries 4, 5 and 6, Table 3), leading to the formation of DMTHF as a principal product.[16] Thus, 220 °C seems to be the optimum temperature to obtain a good yield of DMF after 4 h of reaction with this catalyst.

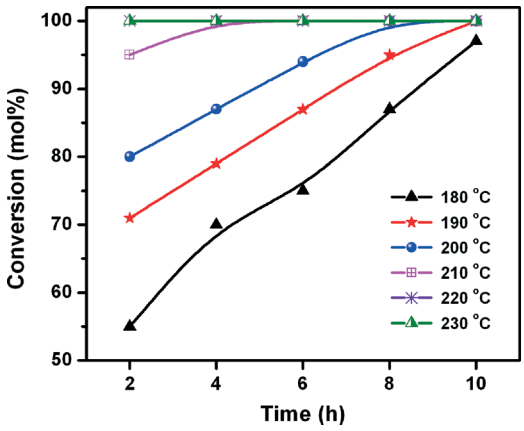

Fig. 5 Effect of reaction temperature on HMF conversion as a function of reaction time. Reaction conditions: HMF (1 mmol, 126 mg); catalyst (RH-1, 50 mg); H_2 pressure (10 bar); solvent (2-propanol, 25 mL); stirring speed (500 rpm).

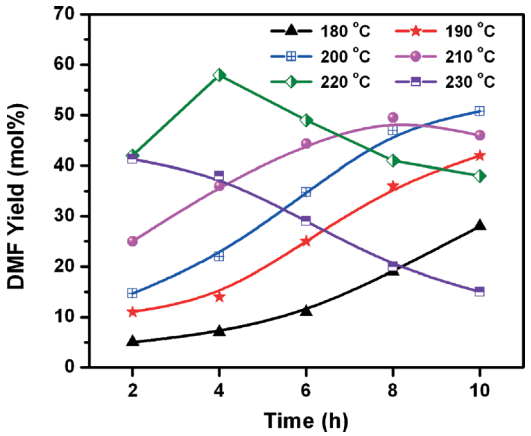

Fig. 6 Effect of reaction temperature on DMF yield as a function of reaction time. Reaction conditions: HMF (1 mmol, 126 mg); catalyst (RH-1, 50 mg); H_2 pressure (10 bar); solvent (2-propanol, 25 mL); stirring speed (500 rpm).

2.2.2. Effect of solvent. The effect of solvent on the catalytic activity in the liquid-phase hydrogenolysis of HMF to DMF was investigated over the RH-1 catalyst at 220 °C and at 7 bar H_2 pressure. Solvents of different chemical nature, such as protic (2-propanol), aprotic polar (tetrahydrofuran (THF) and 1,2-dimethoxyethane (1,2-DME)) and non-polar (toluene) solvents, were used to investigate the influence of solvent on hydrogenolysis activity and DMF selectivity. The results given in Fig. 7 clearly show that the RH-1 activity is heavily solvent dependent. It can be seen that the catalytic activity follows the order: 2-propanol > THF ≈ 1,2-DME > toluene. The lower HMF hydrogenolysis activity in toluene could be explained on the basis of the competitive adsorption between the reactant and the solvent on the active catalytic sites. Moreover, with toluene as a solvent, hydrogenated compounds of toluene were observed under the reaction conditions studied. Competitive adsorption between toluene and HMF on the active catalytic sites results in reduced availability of active sites for HMF. As a result, the hydrogenolysis activity of HMF drops down. The strength of toluene adsorption is controlled by the degree of overlap of the carbon π molecular orbitals with the d bands of the Ru metal.[30]

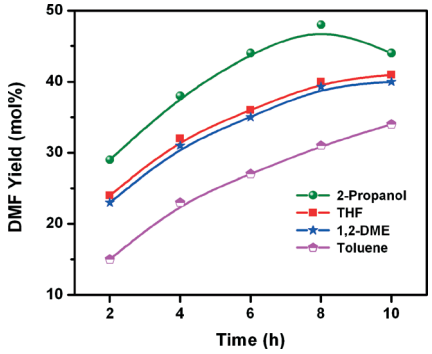

Fig. 7 Effect of solvent on DMF yield as a function of reaction time. Reaction conditions: HMF (1 mmol, 126 mg); catalyst (RH-1, 50 mg); temperature (220 °C); solvent (25 mL); H_2 pressure (7 bar); stirring speed (500 rpm).

To understand the reason behind the superior activity in the presence of 2-propanol, experimental runs were carried out in the absence of H_2 at 220 °C under 5 bar N_2 pressure over RH-1, RH-2, RH-3 and RH-imp catalysts (Fig. S1, ESI†). Catalyst RH-1 exhibited superior activity in terms of CTH, compared to other catalysts, probably due to the smaller Ru crystallite size. The results of the CTH experiments, using RH-1 in the absence of H_2, with different solvents are given in Fig. 8. About 14 mol% DMF yield was seen after 5 h of reaction with 2-propanol as a solvent. Acetone was detected as one of the products in this experiment, implying hydrogen transfer from 2-propanol. However, the 2-propanol consumed for the purpose of CTH was low (<1 mol%), as it was used as a solvent at a high solvent-to-substrate molar ratio (>300). No CTH was seen when THF or 1,2-DME was used as a solvent under similar conditions. These results strongly suggest that in 2-propanol, HMF is hydrogenated over the RH-1 catalyst *via* an additional reduction mechanism involving hydrogen transfer from 2-propanol to HMF in the presence of the Ru metal catalyst.[30] Thus, HMF is hydrogenated by molecular H_2 as well as by hydrogen transfer from 2-propanol over the catalyst (Fig. S2, ESI†). However, the rate of HMF hydrogenation using molecular H_2 is comparatively much higher than

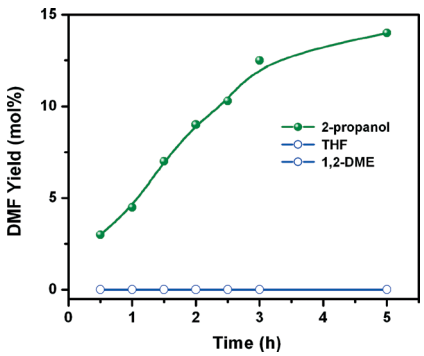

Fig. 8 CTH of HMF as a function of reaction time over the RH-1 catalyst. Reaction conditions: HMF (1 mmol, 126 mg); catalyst (50 mg); temperature (220 °C); solvent (25 mL); N_2 pressure (5 bar); stirring speed (500 rpm).

that of CTH (difference in DMF yield in Fig. 7 and 8). To understand this aspect further, the effect of temperature, the effect of Ru content and the effect of H_2 pressure were investigated with THF as a solvent, which is not expected to be reactive in the given conditions. These results are given in the ESI (Fig. S3, S4 and S5†). Unlike with 2-propanol, variation of any of the reaction parameters did not lead to a change in DMF yield, clearly demonstrating the advantage of 2-propanol as a solvent. In view of the higher apparent catalytic activity and superior DMF yield, 2-propanol was chosen as the solvent for further investigations. It is well known that there are differences between heterogeneous catalytic hydrogenation using hydrogen donor molecules as the source of hydrogen and hydrogenation using molecular H_2.[31] The CTH reaction could occur through direct hydride transfer from 2-propanol to HMF. Further investigations are required to delineate the mechanism for hydrogenolysis using 2-propanol as the hydrogen source.

Compounds: 5-hydroxymethylfurfural (HMF); 2,5-bis(hydroxymethyl)furan (BHMF); 5-methyl furfural (MF); 5-methyl furfuryl alcohol (MFA); furfuryl alcohol (FA); 2,5-bis(hydroxymethyl)tetrahydrofuran (BHMTHF); 5-methyl-tetrahydrofurfuryl alcohol (MTHFA); 5,5′-(oxybis(methylene))-bis(2-methylfuran) (OMBM); 2,5-dimethylfuran (DMF); *cis*-2,5-dimethyltetrahydrofuran (*cis*-DMTHF); 2-methylfuran (MFU); *trans*-2,5-dimethyltetrahydrofuran (*trans*-DMTHF); 2-methyl-tetrahydrofuran (MTHF).

2.2.3. Effect of Ru metal content of catalysts. To optimise the Ru content of the catalyst, a series of catalysts with different wt% of Ru were prepared and evaluated for HMF hydrogenolysis. The HMF conversions and product yields are summarized in Table 2 (Fig. S2, ESI†). Catalyst RH-1 showed the highest activity in terms of HMF hydrogenolysis, yielding 58 mol% DMF at 100 mol% HMF conversion (entry 1, Table 2). However, under similar reaction conditions, DMF yields were only 48, 35 and 45 mol% over RH-2, RH-3 and RH-imp catalysts, respectively. When Ru content was low (RH-1 with 0.56 wt% Ru), smaller yields of the hydrogenated products, BHMF and DMF, were observed, leading to high yield of DMF. On the other hand, over catalysts with high Ru content (RH-2 and RH-3), a significant increase in the yields of ring hydrogenated products such as 2,5-bis(hydroxymethyl)tetrahydrofuran (BHMTHF) and DMTHF was observed. This could be a result of the larger Ru crystallite size in these catalysts (Table 1). However, the metal surface areas of RH-2 and RH-imp were higher than that of RH-1 (Table 1). Even then, RH-1 was found to be superior, as the smaller crystallite size (2.8 nm) suppresses ring hydrogenation, thus leading to a better DMF yield over RH-1. This is a welcome result, as the hydrotalcite catalyst with low Ru content (RH-1) can achieve a high DMF yield (58 mol%), which may be helpful for the economic production of transportation fuels from biomass.

To ascertain the desirability of Ru in the catalyst, HMF hydrogenolysis was carried out in its absence, using only HT_{cal}, which gave <1 mol% DMF yield (entry 5, Table 2).

Table 2 Product distributions during HMF hydrogenolysis over different catalysts[a]

Entry	Catalyst	HMF conv. (mol%)	Yield (mol%) DMF	DMTHF	BHMF	MFA	MF	BHMTHF	MFU	Others[b]	TOF[c] (h^{-1})
1	RH-1	100	58	6	5	8	4	2	3	14 (3)	52.3
2	RH-2	100	48	10	8	11	5	6	1	11 (4)	24.4
3	RH-3	92	35	9	8	8	4	15	2	11 (7)	10.4
4	RH-imp	100	45	8	7	12	4	7	2	15 (4)	39.0
5	HT_{cal}	32	<1	0	1	1	0	0	0	29 (29)	—
6	none	8	0	0	0	0	0	0	0	8 (8)	—

[a] Reaction conditions: HMF (1 mmol, 126 mg); catalyst (50 mg); temperature (220 °C); H_2 pressure (10 bar); solvent (2-propanol, 25 mL); reaction time (4 h); stirring speed (500 rpm). [b] It includes 5-methyltetrahydrofurfuryl alcohol (MTHFA), furfuryl alcohol (FA), 5,5′-(oxybis(methylene))bis(2-methylfuran) (OMBM), 2,5-bis(hydroxymethyl)tetrahydrofuran (BHMTHF) and other unidentified products (condensation products, values in brackets correspond to the unidentified products). [c] TOF = turnover frequency (moles of DMF produced per mole of Ru).

Blank experiments with HMF in 2-propanol, in the absence of a catalyst, showed no activity for DMF formation (entry 6, Table 2). But, minor amounts of by-products, probably as a result of HMF polymerization and condensation reactions, were observed in the absence of the catalyst.

2.2.4. Effect of H_2 pressure. The influence of H_2 pressure on the HMF hydrogenolysis was studied by varying the pressure in the range of 1–13 bar. Results of these experiments are given in Fig. 9. When the reaction was carried out in the low pressure range (1 to 7 bar), the intermediate products such as BHMF, MFA and MF formed in significant quantities, showing that the hydrogenolysis was incomplete. As a result, only 48 mol% DMF yield was obtained even after 8 h of reaction under 7 bar H_2 pressure. On increasing the H_2 pressure to 10 bar, the DMF yield reached the maximum (58 mol%) over the RH-1 catalyst within 4 h of reaction. But, the DMF yield decreased on continuation of the reaction for further duration (Fig. 9 and entry 3, Table 3). Similarly, increasing the H_2 pressure further to 13 bar has an adverse affect on the DMF yield, mostly due to the increased rate of consecutive ring hydrogenation of DMF, leading to the formation of DMTHF in significant quantities (entries 8, 9 and 10, Table 3). Moreover, the concentration of other unwanted by-products such BHMTHF and 5-methyltetrahydro-furfuryl alcohol (MTHFA) increased at higher pressure (13 bar). These results clearly show that at higher H_2 pressures, ring hydrogenation is the predominant reaction, leading to the lower yield of DMF (Table 3). Hence, 10 bar of H_2 pressure was found to be the optimum, which was used for further investigations.

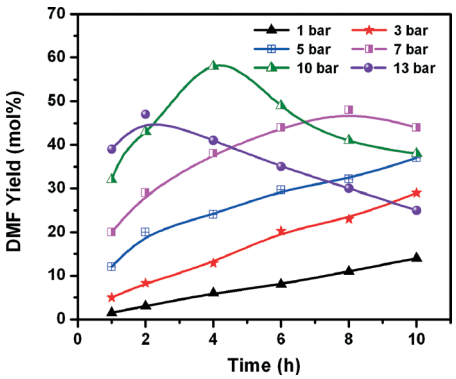

Fig. 9 Effect of H_2 pressure on DMF yield as a function of reaction time. Reaction conditions: HMF (1 mmol, 126 mg); catalyst (RH-1, 50 mg); temperature (220 °C); solvent (2-propanol, 25 mL); stirring speed (500 rpm).

2.2.5. Effect of catalyst content. The amount of catalyst used in the reaction is an important parameter that needs to be optimized to get high DMF yield. Experiments were conducted by varying the amount of the RH-1 catalyst from 15 to 70 mg at 220 °C, while maintaining the same substrate content (Fig. 10). These experiments showed that the DMF yield increased initially with catalyst content. When the catalyst was 15 mg, the DMF yield reached a maximum of 40 mol% after 12 h of reaction, which declined on further increasing the reaction time. When 30 mg of catalyst was used, the DMF yield reached 46 mol% in a slightly shorter duration (10 h) of reaction time. With 50 mg of catalyst, a maximum DMF yield of 58 mol% was accomplished only in 4 h of reaction time, but it decreased when the reaction was continued further, mostly due to ring hydrogenation of DMF. However, when the catalyst content was further increased to 70 mg, a much lower DMF yield of 44 mol% was achieved, which decreased with further increasing time on stream. These results show that with increased duration of reaction even at low catalyst content, DMF undergoes consecutive hydrogenation, leading to DMTHF formation. At higher catalyst content, more active sites are available, which drive the formation of side products such as MFU and MTHF in addition to hydrogenated products MTHFA and DMTHF, leading to a lower DMF yield. Hence, optimization of catalytic sites and reaction time is essential to obtain the maximum DMF yield. Based on these studies, 50 mg of catalyst was found to be the optimum under the given reaction conditions.

2.2.6. Proposed reaction pathway. To understand the reaction network of hydrogenolysis of HMF to DMF, studies were carried out at lower temperature (180 °C) while monitoring the products as a function of time using the RH-1 catalyst. The results are shown in Fig. 11. When the reaction time was increased from 1 to 10 h, the conversion of HMF increased from 40 to 97 mol% and the concentration of the products changed in a complex manner. The yield of DMF increased

Table 3 Effect of reaction temperature and hydrogen pressure on DMTHF yield[a]

Entry	Time (h)	Temp (°C)	DMF yield (mol%)	DMTHF yield (mol%)	*Cis* : *trans* ratio of DMTHF
1	4	210	36	3	6.3
2	4	220	58	6	6.2
3	6	220	49	15	6.7
4	4	230	38	17	6.6
5	6	230	29	26	6.4
6	8	230	20	32	6.5
7[b]	4	220	38	2	6.1
8[c]	2	220	47	7	6.8
9[c]	4	220	41	12	6.6
10[c]	6	220	35	21	6.6
11[d]	4	220	30	19	6.7

[a] Reaction conditions: HMF (1 mmol, 126 mg); catalyst (RH-1, 50 mg); H_2 pressure (10 bar); solvent (2-propanol, 25 mL); stirring speed (500 rpm). [b] H_2 pressure (7 bar). [c] H_2 pressure (13 bar). [d] H_2 pressure (16 bar).

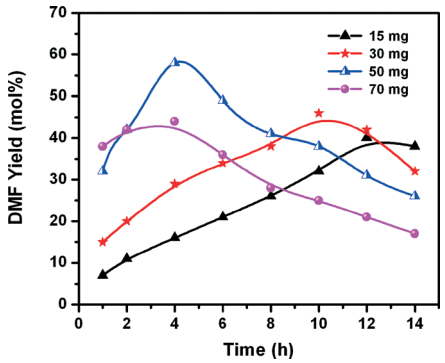

Fig. 10 Effect of catalyst content on DMF yield as a function of reaction time over the RH-1 catalyst. Reaction conditions: HMF (1 mmol, 126 mg); temperature (220 °C); H_2 pressure (10 bar); solvent (2-propanol, 25 mL); stirring speed (500 rpm).

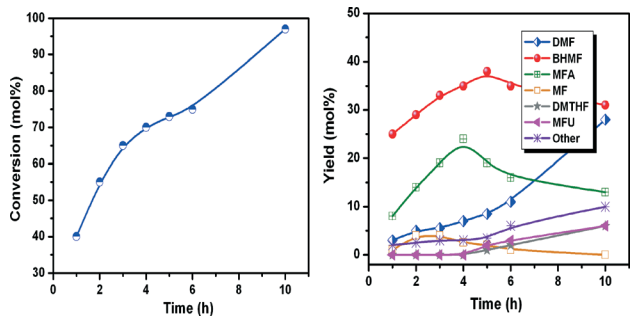

Fig. 11 Conversion of HMF and product yields as a function of time at 180 °C. Left: conversion of HMF. Right: yields of various products. Reaction conditions: HMF (1 mmol, 126 mg); catalyst (RH-1, 50 mg); H_2 pressure (10 bar); solvent (2-propanol, 25 mL); stirring speed (500 rpm).

continuously with reaction time, while the yield of BHMF reached a plateau at 38 mol% after 5 h and then decreased with increasing reaction time. The MFA yield also showed a similar trend to that of BHMF, passing through the maximum at 4 h. Though MF, DMTHF and MFU were also observed in the product, their yields were low during the entire duration of the reaction. The low yield of MF may be attributed to the fact that it does not form fast enough. Based on these results, a reaction network of the hydrogenolysis of HMF to DMF is proposed (Scheme 1).

To validate the proposed reaction sequence in Scheme 1, hydrogenolysis experiments were conducted with MF as the starting substrate. The results (Fig. 12) demonstrate that MF was quite reactive. Within 3 h of reaction time, this intermediate was converted principally to MFA and DMF. With increasing reaction time, the yield of MFA decreased but the DMF yield increased. The results of this experiment show that the rate of MF hydrogenation to MFA is fast, with the subsequent hydrogenolysis of MFA to DMF being very rapid. Low yields of DMTHF and MFU were also observed, whose concentration increased with time followed by the formation of DMF.

The *cis*- and *trans*-DMTHF isomers have different physical properties, *e.g.* boiling points, which can be distinguished and quantified by GC-FID. Our experiments show that the formation of *cis*-DMTHF is favoured over *trans*-DMTHF, with a *cis* : *trans* molar ratio of ≈6.5 : 1 under the given experimental conditions (Table 3). This may be explained in terms of steric crowding. During the course of the reduction reaction, addition of the second hydrogen molecule takes place on the same face as the first would result in less steric hindrance, whereas the hydrogen molecule may be sterically crowded by the methyl group, restricting the formation of *trans*-DMTHF (Scheme 2).

2.2.7. Recyclability of the catalyst. Catalyst recyclability is of great importance in order to apply the best found catalytic system and convert it into an industrial process. The recyclability of the RH-1 catalyst was evaluated by repeating the reaction with the same catalyst at least five times without any regeneration/activation (Fig. 13 and S7, ESI†). The results show that the catalyst remains active even after five cycles, though a minor drop in DMF yield was observed probably due to blockage of some catalytic sites. However, on regeneration by calcination–reduction steps, 100% activity was restored. These results indicate good stability of the catalyst. The product mixture at the end of each recycle was analyzed

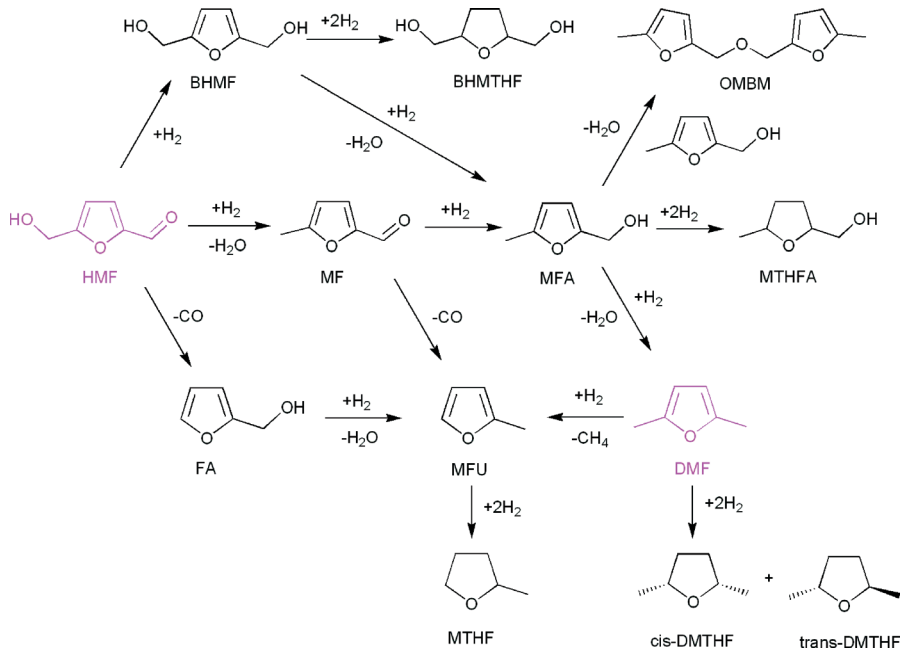

Scheme 1 Reaction network of the hydrogenolysis of HMF to DMF over the RH-1 catalyst.

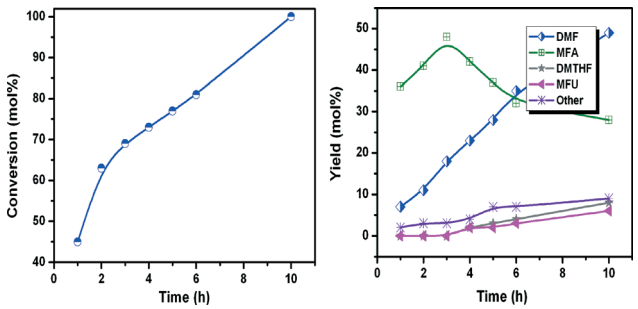

Fig. 12 Conversion of MF and product yields as a function of time at 180 °C. Left: conversion of MF. Right: yields of various products. Reaction conditions: MF (1 mmol, 110 mg); catalyst (RH-1, 50 mg); H_2 pressure (10 bar); solvent (2-propanol, 25 mL); stirring speed (500 rpm).

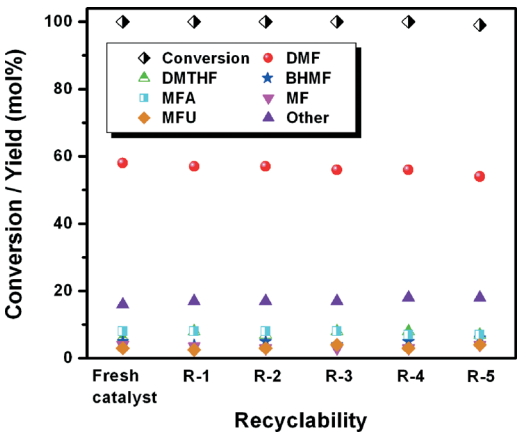

Fig. 13 The recyclability experiments of the RH-1 catalyst in HMF hydrogenolysis. Reaction conditions: solvent (2-propanol, 25 mL); molar ratio of HMF to Ru (360); temperature (220 °C); H_2 pressure (10 bar); reaction time (4 h); stirring speed (500 rpm).

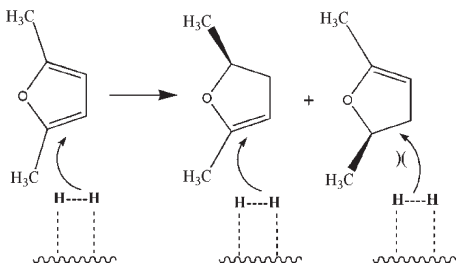

Scheme 2 Mechanism for the preferential formation of the *cis*-DMTHF isomer over the *trans*-DMTHF isomer from DMF over the RH-1 catalyst.

by ICP-OES, for the presence of any Ru due to leaching out of the catalyst. No such leaching was observed. Moreover, the concentration of Ru in the catalyst was similar to that of the starting catalyst even after five cycles.

3. Conclusions

The present investigations demonstrate that highly dispersed Ru-containing mixed metal oxide catalysts can be obtained by the calcination of hydrotalcite-like precursors, which were obtained through co-precipitation. As a result, even catalysts with low Ru metal (0.56 wt%) content were highly active in the conversion of HMF to DMF. The possible reaction pathway for the conversion of HMF to DMF was explored by using the intermediate compound MF as a starting material.

Analysis of intermediate products at different stages of reaction showed that DMF is formed *via* BHMF followed by MFA. Under optimized reaction conditions, a maximum DMF yield of 58 mol% was achieved at 220 °C, at 10 bar H_2 pressure with 2-propanol as the solvent. The catalyst can be recycled without any significant loss in activity. Higher DMF yields were seen with 2-propanol as the solvent, as a result of hydrogen transfer from 2-propanol to HMF over the Ru metal. This study clearly shows that Ru-containing mixed metal oxide-derived catalysts have excellent potential for the conversion of biomass oxygenates to biofuels.

4. Experimental section

4.1. Chemicals

All the chemicals were reagent grade and used without further purification. HMF (99%), DMF (99%), DMTHF (99%), MFU (99%), MTHF (99%) and THF (98%) were procured from Sigma-Aldrich. MF (99%) and $Ru(NO)(NO_3)_3$ were purchased form Alfa Aesar, while $Mg(NO_3)_2{\cdot}6H_2O$, $Al(NO_3)_3{\cdot}9H_2O$, toluene, 2-propanol and 1,2-dimethoxyethane were purchased from Loba Chemicals, India.

4.2. Preparation of catalysts

Ruthenium-doped HT catalyst precursors were prepared by the co-precipitation method at a constant pH of 9.5–10. In a typical synthesis, an aqueous solution containing $Mg(NO_3)_2{\cdot}6H_2O$ (0.25 mol), $Al(NO_3)_3{\cdot}9H_2O$ (0.25 mol) and $Ru(NO)(NO_3)_3$ (1.5 wt%, Ru content 15 mg mL^{-1}) was prepared in 50 mL of double distilled deionized water. This solution was added dropwise to a second solution containing Na_2CO_3 (0.125 M) in 50 mL of double distilled deionized water under vigorous stirring at 30 °C. The pH of the mixture was maintained constant while adding aqueous 0.25 M NaOH. The precipitate formed was filtered, washed thoroughly and dried at 100 °C for 10 h. Subsequently, it was calcined in air at 450 °C for 4 h followed by reduction in H_2 stream (30 mL min^{-1}) at 350 °C for 3 h. These samples with different Ru contents were designated as RH-1, RH-2 and RH-3. A similar procedure was adopted for the preparation of the Mg–Al HT sample with a Mg/Al mole ratio of 3, without using $Ru(NO)(NO_3)_3$ solution. The Ru-impregnated catalyst (RH-imp) was prepared by the pore filling dry impregnation method. For this, an aqueous solution of $Ru(NO)(NO_3)_3$ was added dropwise to the freshly dried HT sample. The resultant wet solid was initially dried at ambient temperature for 12 h and subsequently dried at 100 °C for 10 h. Finally, the catalyst was calcined in air at 450 °C for 4 h followed by reduction in H_2 (30 mL min^{-1}) at 350 °C for 3 h.

4.3. Characterization techniques

The physico-chemical characterization of the catalyst and support was carried out by X-ray diffraction (XRD), scanning electron microscopy (SEM), transmission electron microscopy (TEM), temperature-programmed reduction (TPR), *etc.* The X-ray diffraction patterns were obtained using a PANalytical X'Pro dual goniometer equipped with an X'celator solid state detector. Nickel filtered Cu Kα (λ = 1.5406 Å, 40 kV, 30 mA) radiation was used and the data collection was carried out using a flat holder in Bragg–Brentano geometry. The data were recorded in the 2θ range of 5–90° with 0.02° step size. The surface areas of all the samples were investigated by N_2 sorption at −196 °C (Quanta chrome Autosorb IQ). Prior to sorption, the samples were evacuated at 200 °C for 3 h to a residual pressure of 2×10^{-3} torr. The isotherms were analyzed in the relative pressure (p/p_o) range of 0.05 to 0.30. Hydrogen chemisorption was also conducted using a Quantachrome autosorb iQ instrument. Before chemisorption at 40 °C, the catalyst was reduced *in situ* in H_2 flow at 350 °C. The amount of Ru present in the samples was estimated by ICP-OES (Spectro Arcos, FHS-12). The SEM images of the samples were recorded using a JEOL-JSM-5200 to study the morphology. The samples were prepared by dispersing them ultrasonically in isopropyl alcohol and transferring a portion of it onto a silicon wafer, and then subsequently dried and gold coated before study. TEM images were collected using a FEI Technai TF-30 instrument operating at 300 kV. The samples for TEM measurement were prepared by placing a droplet of the highly diluted suspension of the sample in isopropyl alcohol on a carbon-coated copper grid and allowing to dry at room temperature. TPR studies of the catalysts were carried out using a Micromeritics Autochem-2920 instrument in the temperature range 50–600 °C at a heating rate of 5 °C min^{-1} using 5% H_2 in He as the probe gas. The H_2 consumption in the TPR study was estimated quantitatively by a thermal conductivity detector that was calibrated before the TPR study. Prior to the TPR, the catalyst was pre-treated at 300 °C for 1 h using 5% oxygen in a helium gas mixture.

4.4. Evaluation of catalysts

Evaluation of catalysts was carried out using a 100 mL capacity Parr autoclave (SS316). In a typical experiment, 1 mmol (126 mg) of HMF, 25 mL of solvent and the required amount of the freshly reduced catalyst were introduced into the reactor vessel. After closing the reactor, it was purged two to three times with hydrogen and filled with the same gas to the required hydrogen pressure. Subsequently, the reaction vessel was heated under stirring to the required temperature. During the reaction, the liquid samples were withdrawn periodically and analyzed by a GC (Agilent 7890A) equipped with a flame ionization detector and a CP Sil 8 CB capillary column (30 m length, 0.25 mm diameter). Product identification was done using authentic standards and by using GC-MS (Varian, Saturn 2200).

Acknowledgements

Atul S. Nagpure and Ashok Kumar acknowledge the Council of Scientific and Industrial Research, New Delhi, for providing

a senior research fellowship. The authors also acknowledge financial support from CSIR Network project CSC-0122.

References

1 G. W. Huber, S. Iborra and A. Corma, *Chem. Rev.*, 2006, **106**, 4044.
2 A. Corma, S. Iborra and A. Velty, *Chem. Rev.*, 2007, **107**, 2411.
3 J. N. Chheda, G. W. Huber and J. A. Dumesic, *Angew. Chem., Int. Ed.*, 2007, **46**, 7164.
4 K. Shimizu and A. Satsuma, *Energy Environ. Sci.*, 2011, **4**, 3140.
5 E. L. Kunkes, D. A. Simonetti, R. M. West, J. C. Serrano-Ruiz, C. A. Gärtner and J. A. Dumesic, *Science*, 2008, **322**, 417.
6 A. J. Ragauskas, C. K. Williams, B. H. Davision, G. Britovsek, J. Cairney, C. A. Eckert, W. J. Frederick Jr., J. P. Hallett, D. J. Leak, C. L. Liotta, J. R. Mielenz, R. Murphy, R. Templer and T. Tschaplinski, *Science*, 2006, **311**, 484.
7 B. F. M. Kuster, *Starch*, 1990, **42**, 314.
8 Y. Román-Leshkov, C. J. Barrett, Z. Y. Liu and J. A. Dumesic, *Nature*, 2007, **447**, 982.
9 L. Deng, J. Li, D. M. Lai, Y. Fu and Q. X. Guo, *Angew. Chem., Int. Ed.*, 2009, **48**, 6529.
10 J. Q. Bond, D. M. Alonso, D. Wang, R. M. West and J. A. Dumesic, *Science*, 2010, **327**, 1110.
11 I. T. Horváth, J. Mehdi, V. Fábos, L. Boda and L. T. Mika, *Green Chem.*, 2008, **10**, 238.
12 J. P. Lange, W. D. van de Graaf and R. J. Haan, *ChemSusChem*, 2009, **2**, 437.
13 S. Song, R. Daniel, H. Xu, J. Zhang, D. Turner, M. L. Wyszynski and P. Richards, *Energy Fuels*, 2010, **24**, 2891.
14 T. Thananatthanachon and T. B. Rauchfuss, *Angew. Chem., Int. Ed.*, 2010, **49**, 6616.
15 M. Chidambaram and A. T. Bell, *Green Chem.*, 2010, **12**, 1253.
16 T. S. Hansen, K. Barta, P. T. Anastas, P. C. Ford and A. Riisager, *Green Chem.*, 2012, **14**, 2457.
17 J. M. R. Gallo, D. M. Alonso, M. A. Mellmer and J. A. Dumesic, *Green Chem.*, 2013, **15**, 85.
18 W. Yang and A. Sen, *ChemSusChem*, 2010, **3**, 597.
19 A. Sen and W. Yang, US0307050A1, 2010.
20 W. Yang and A. Sen, *ChemSusChem*, 2011, **4**, 349.
21 S. Morikawa, *Noguchi Kenkyusho Jiho*, 1980, **23**, 39.
22 T. Thananatthanachon and T. B. Rauchfuss, *Angew. Chem.*, 2010, **122**, 6766.
23 S. De, S. Dutta and B. Saha, *ChemSusChem*, 2012, **5**, 1826.
24 D. J. Braden, C. A. Henao, J. Heltzel, C. C. Maravelias and J. A. Dumesic, *Green Chem.*, 2011, **13**, 1755.
25 L. Chen, Y. Zhu, H. Zheng, C. Zhang, B. Zhang and Y. Li, *J. Mol. Catal. A: Chem.*, 2011, **351**, 217.
26 T. Miyazawa, S. Koso, K. Kunimori and K. Tomishige, *Appl. Catal., A*, 2007, **318**, 244.
27 F. Basile, L. Basini, G. Fornasari, M. Gazzano, F. Trifiro and A. Vaccari, *Chem. Commun.*, 1996, 2435.
28 Q. Wang, H. H. Tay, Z. Guo, L. Chen, Y. Liu, J. Chang, Z. Zhong, J. Luo and A. Borgna, *Appl. Clay Sci.*, 2012, **55**, 18.
29 (*a*) R. Lanza, S. G. Jaras and P. Canu, *Appl. Catal., A*, 2007, **325**, 57; (*b*) M. G. Cattania, F. Parmigiani and V. Ragaini, *Surf. Sci.*, 1989, **211**, 1097; (*c*) S.-H. Lee and D. J. Moon, *Catal. Today*, 2011, **174**, 10.
30 N. M. Bertero, A. F. Trasarti, C. R. Apesteguía and A. J. Marchi, *Appl. Catal., A*, 2011, **394**, 228.
31 R. A. W. Johnstone, A. H. Wilby and I. D. Entwistle, *Chem. Rev.*, 1985, **85**, 129.

